PCCP

Accepted Manuscript

This is an *Accepted Manuscript*, which has been through the Royal Society of Chemistry peer review process and has been accepted for publication.

Accepted Manuscripts are published online shortly after acceptance, before technical editing, formatting and proof reading. Using this free service, authors can make their results available to the community, in citable form, before we publish the edited article. We will replace this *Accepted Manuscript* with the edited and formatted *Advance Article* as soon as it is available.

You can find more information about *Accepted Manuscripts* in the Information for Authors.

Please note that technical editing may introduce minor changes to the text and/or graphics, which may alter content. The journal's standard Terms & Conditions and the Ethical guidelines still apply. In no event shall the Royal Society of Chemistry be held responsible for any errors or omissions in this *Accepted Manuscript* or any consequences arising from the use of any information it contains.

ROYAL SOCIETY OF CHEMISTRY

www.rsc.org/pccp

PCCP

ARTICLE

A Fast Self-Cleaning SERS-Active Substrate Based on Inorganic–Organic Hybrid Nanobelts Film

Received 00th January 20xx,
Accepted 00th January 20xx

DOI: 10.1039/x0xx00000x

www.rsc.org/

Rui Hao†, Jie Lin†, Hua Wang,* Bo Li, Fengshi Li, and Lin Guo*

Surface-enhanced Raman scattering (SERS) spectroscopy, as a robust and attractive spectroscopic technique, has been widely used for the unequivocal identification of analytes, and an ideal SERS substrate should be highly sensitive and reproducible. Currently, existing substrates usually exhibit substantial sensitivity, however, achieve their recyclable utilization by multi-steps and complex procedures with the prerequisite of external facilities. Herein, an inorganic–organic hybrid nanobelts film assembled by novel Ag@Ag(DMSO)$_x$Cl nanobelts was proposed as a active SERS substrate. This unique substrate exhibits highly sensitive SERS detection properties, and realizes ultrafast self-cleaning by in-situ photocatalytic degradation of targeted molecules adsorbed to the film during the detection process, showing the potential for the real-time online monitoring. Our study demonstrates a new concept of preparing in-situ self-cleaning substrate by rational designing and assembling of special nanomaterials.

Introduction

Surface-enhanced Raman scattering (SERS) spectroscopy is a robust and attractive spectroscopic technique used for the unequivocal identification of analytes.[1-4] Considering potential application of the SERS detection as a generally analytical tool, it is necessary to develop low-cost, highly efficient SERS substrates which can afford strong enhancement factors, stability[5] and reproducibility.[6, 7] Although most of the conventional SERS substrates using noble metal nanoparticles exhibit highly sensitive and stable, they suffer from poor recyclability. Currently, great efforts have been devoted to explore the hybrids of semiconductor metal oxide[8-11] and noble metal,[12-14] such as ZnO/Ag, TiO_2/Au and Fe_3O_4@C@Ag core-shell structures,[6, 15-18] as high efficient and recyclable SERS-active substrates. However, recycle procedures they proposed are usually multi-steps and complex with the prerequisite of external facilities such as high-power UV light source or magnetic force. Thus, an ideal SERS substrate should not only retain highly sensitive SERS detection to organic molecules, but also achieve their recyclable utilization facilely.

For highly sensitive SERS detection application, silver nanoparticles are often selected due to their unique and tunable optical properties derived from the strong surface plasmonic resonance (SPR) effects.[19-23] Meanwhile, plasmonic Ag nanoparticles may serve as alternative sensitizers to enhance the light absorption of semiconductors in the visible region, and the resulting hybridized photocatalysts can maintain stability and deliver high activities. Many studies have indicated that silver/silver compounds (Ag/AgX, X=Cl, Br, PO_3) possess high efficient and stable photocatalytic properties under visible light irradiation.[24-31] Thus, Ag/AgX composites could not only detect the targeted organic molecules, but also photodegrade them. On the other hand, for creating recyclable application of SERS detection substrates, integrating the active materials on a chip or assembling them to form a macroscopic film is feasible.[32] As we known, one-dimensional (1D) nanostructures are easily to construct free-standing architectures for practical applications, while maintaining the intrinsic features of individual 1D nanostructures for a variety of engineering applications.[33-36] From this, it can be expected that a free-standing film assembled by one-dimension (1D) Ag/AgX nanomaterials could be used as a highly sensitive SERS substrate, and facilely achieve the recyclable utilization by in-situ self-cleaning during the detection process.

Herein, Ag@Ag(DMSO)$_x$Cl nanobelts have been successfully prepared by a facile wet-chemical method for the first time. Using this unique 1D nanostructure, a free-standing film has been fabricated by a following liquid filtration method.[37] Being as an active substrate, the film exhibits highly sensitive SERS detection properties. Simultaneously, the material can achieve ultrafast self-cleaning by photocatalytic degradation of targeted molecules adsorbed to the film under the laser irradiation while SERS detection, and thus realize the renewability spontaneously. Our work not only provides a high efficient recyclable SERS-active substrate, but also proposes a

School of Chemistry and Environment, Beihang University, Beijing 100191, PR China.
E-mail: wanghua8651@buaa.edu.cn; guolin@buaa.edu.cn.
†These authors contributed equally to this work.
Electronic Supplementary Information (ESI) available: [SEM images of the samples prepared with varied reaction condition; AFM, TEM, SAED, TG, DRS of as-prepared Ag@Ag(DMSO)$_x$Cl nanobelts; The laser power and laser wavelength dependence of the R 6G SERS signals; Raman spectra of pure R6G and MB dye molecules]. See DOI: 10.1039/x0xx00000x

Physical Chemistry Chemical Physics Accepted Manuscript

new strategy for designing and fabricating it by rationally taking advantage of as-prepared nanomaterials.

Experimental

Preparation of Ag@Ag(DMSO)xCl nanobelts: The Ag@Ag(DMSO)xCl nanobelts were prepared through a facile precipitation reaction. Typically, 54 mg of Polyvinyl pyrrolidone (PVP) (average MW 58000, K29-32, Acros) and 0.768 g NaCl were added to dimethyl sulfoxide (DMSO)/distilled water (30 mL, 20/10, V/V), followed by intensive magnetic stirring at 60 ºC for 30 min. Subsequently, 12 mL aqueous solution of CH_3COOAg (57 mg) was dropwise added to the mixed solution.

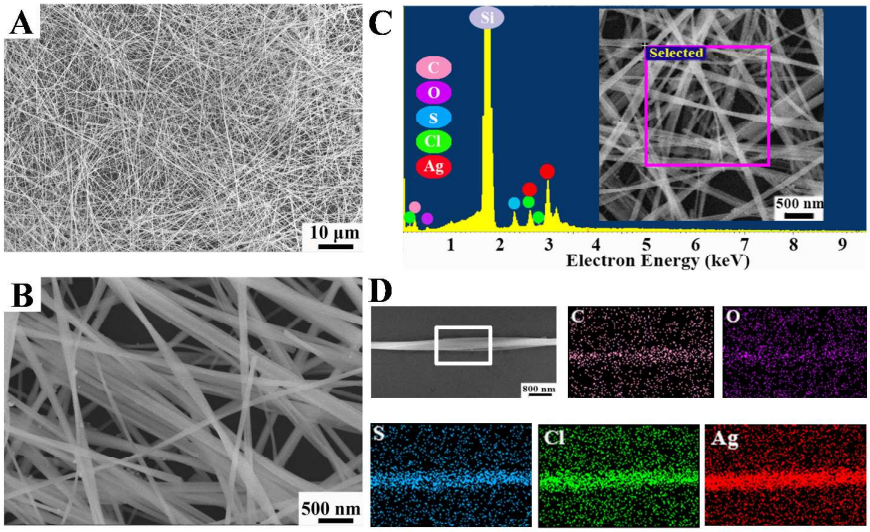

Fig. 1 SEM images (A, B) of Ag@Ag(DMSO)$_x$Cl nanobelts with different magnification. EDS spectrum (C) of Ag@Ag(DMSO)$_x$Cl nanobelts. (D) SEM image of a single Ag@Ag(DMSO)$_x$Cl nanobelt and elemental mapping of an elected region, indicating spatial distribution of Ag, Cl, S, C and O.

The mixture was kept for another 30 min at 60 ºC for an adequate precipitation process and then transferred into a 45mL Teflon-lined stainless steel autoclave, heated at 140 ºC for 2 h. The products were collected by centrifugation and washed with distilled water and ethanol several times, and finally dried overnight at 60 °C under vacuum condition.

Characterization: The morphologies of the samples were carried out on a JEOL JSM-7500F cold-field emission scanning electron microscope with affiliated energy dispersive X-ray diffraction spectroscopy (EDS). The X-ray diffraction (XRD) spectra of the samples were recorded by a Rigaku Dmax 2200 X-ray diffractometer with Cu Kα radiation (λ=1.5416 Å). FTIR measurements were performed using a Bruker Vertex 70V instrument. The XPS measurements were carried out in a Thermo Scientific ESCALAB 250 XPS system. The spectra for the sample was calibrated by setting the measured BE of C 1s to 284.6 eV and analyzed using X-peak software. The thermal stability was investigated by a thermo-gravimetric instrument (TGA, Netzsch Sta449F3) under nitrogen condition at a heating rate of 10 °C/min. Diffuse reflectance absorption (DRS) spectra of Ag@Ag(DMSO)xCl nanobelts were recorded in the range from 300 to 800 nm using a Hitachi U-3010 spectroscopy with $BaSO_4$ as reference.

Photocatalytic Experiment: Photocatalytic activities of the as-prepared photocatalyst were evaluated by degradation of Rhodamine 6G (R6G) and Methylene Blue (MB) under 300 W Xe lamp with UV cutoff filter (providing visible light with λ≥400 nm). R6G and MB solutions (50 mL, 10-5 mol·L-1) containing 50 mg of the photocatalysts were placed in two 100 mL cylindrical quartz vessels, respectively. Before the light was turned on, the suspension were stirred in dark for 30 min to ensure an adsorption/desorption equilibrium between the catalysts and organic dyes. The degradation of dyes was monitored by UV/Vis spectroscopy (Hitachi U-3010 spectroscopy).

SERS Detection Measurement: the suspension of Ag@Ag(DMSO)$_x$Cl nanobelts was deposited on a ultra-clean silicon plate and dried at room temperature. Then the substrate was immersed into 10^{-5} M R6G ethanol solution 30 min to ensure the absorption equilibrium. After thoroughly being rinsed with absolute ethanol several times to remove the free R6G molecules, the substrate was subjected to Raman characterization. Raman spectra were measured with a confocal micro-Raman spectrometer (Jobin Yvon, HR800) through a 50x (NA=0.75) microscope objective. The Ar-Kr ions laser emitting at a wavelength of 633 nm was used as a source of excitation and the laser power is 1.5 mW. Similar procedures were repeated with 10^{-5} M MB. For comparison, the standard Raman spectra of solid R6G and MB sample was also measured. Lastly, the SERS detection measurement of R 6G molecule was carried out under different laser power and laser wavelength.

Recyclable in-situ SERS Detection: A free-standing film used as SERS detection, was fabricated by a suction filtration method,

This journal is © The Royal Society of Chemistry 20xx

Please do not adjust margins

Physical Chemistry Chemical Physics Accepted Manuscript

then it was cut into small pieces of triangle and fixed on marked silicon for accurate in-situ monitoring by simply dropping dye solutions. After treating with targeted molecules, the SERS signals were collected every 10 s, and the process was repeated five times.

Results and discussion

In a typical synthesis, the Ag@Ag(DMSO)$_x$Cl nanobelts were prepared *via* a directly precipitation reaction, by using H_2O and dimethyl sulfoxide (DMSO) as mixture solvent, and polyvinyl pyrrolidone (PVP) as surfactant as well as the CH_3COOAg as metal precursors. The plausible growth mechanism is a dissolution and recrystallization process, and several factors play synergetic roles for the successful preparation of Ag@Ag(DMSO)$_x$Cl nanobelts (Fig. S1-S4). Fig. 1 A and B is a typical scanning electron microscope (SEM) image of the as-prepared sample, and it can be seen that the product is composed of ultralong 1D nanostructues, which are at least several hundred micrometers in length. The magnified images further reveal that they are nanobelts with 150-300 nm in width and ~70 nm in thickness (Fig. S5). The energy dispersive X-ray diffraction spectroscopy (EDS) spectra (Fig. 1 B) reveal the compound contains the elements of Ag, Cl, S, O and C, areaelectron diffraction (SAED) pattern, which depicts the well-defined diffraction spots, demonstrating the Ag(DMSO)xCl is single crystalline structure and pure phase (Fig. S5). Thus, the Ag compound should be a coordination of a large amount of anions interaction with the AgCl. An Fourier transformed infrared (FTIR) spectrum shows that the vibration bands of -CH_3, C-S, and S=O, suggesting the existence of DMSO in the product (Fig. 2B).[38] Thermal gravimetric analysis (TGA) shows that ~4.2 wt % DMSO remained in the sample, and after removal of the amine at elevated temperature will result in the formation of pure phase AgCl product (Fig. 2C and Fig. S6, S7). The corresponding XPS spectra providing further structural information for as-prepared nanobelts product, and the full spectrum (Fig. 2D) reveals the coordination contains the elements of Ag, Cl, S, O and C, which is consistent with the EDS results. High-resolution XPS spectra of Ag region (Fig. 2E) shows that the weak XPS peaks at 367.7 and 373.7 eV are assigned to Ag(0) $3d_{5/2}$ and $3d_{3/2}$, suggesting the existence of a trace amount of Ag, while the peaks at 367.4 and 373.4 eV assigned to Ag(I) $3d_{5/2}$ and $3d_{3/2}$ exhibit apparent negative shift, demonstrating the electronic effect of Ag and DMSO anions. The binding energies of Cl $2p_{1/2}$ and Cl $2p_{3/2}$ are approximately 199.7 and 198.1 eV, respectively (Fig. 2F).[39]
The color of as-prepared Ag@Ag(DMSO)$_x$Cl nanobelts is grey,

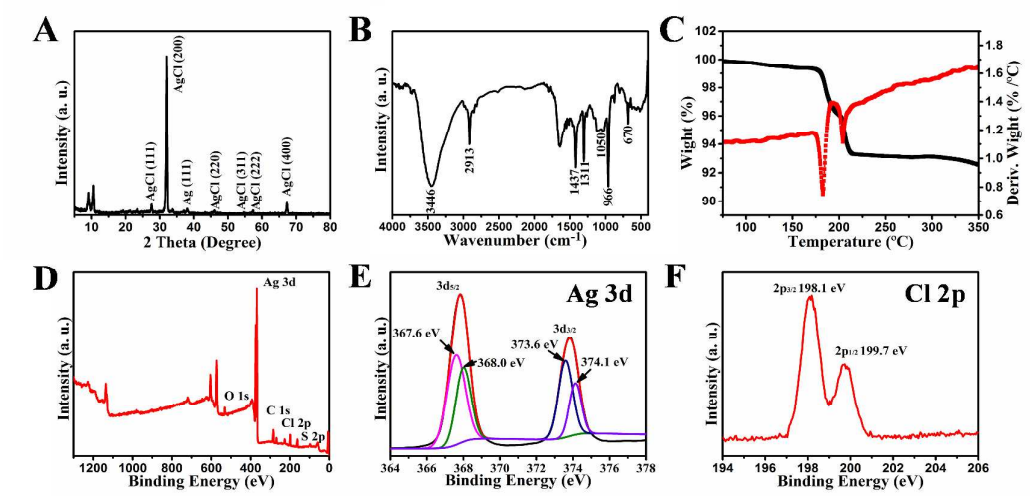

Fig. 2 XRD pattern (A), FTIR spectrum (B), TG and DTG curves (C) of Ag@Ag(DMSO)$_x$Cl nanaobelts. The full (D) and high-resolution XPS spectra of Ag 3d (E) and Cl 2p (F) regions for Ag@Ag(DMSO)$_x$Cl nanobelts.

which are located uniformly throughout the nanobelts and overlapped with each other with no impurity phase segregation at microscale or nanoscale (Fig. 1D).
More optical and photoelectron spectroscopes were utilized to further study the component and structure of as-prepared nanobelt product (Fig. 2). The reflections in the large angle region more than 20° can be readily indexed to cubic phase of AgCl structure and a trace of Ag, and the peaks derived from AgCl exhibit a little positive shift (Fig. 2A). Meanwhile, the peaks in the low angle region smaller than 20° corresponds the large lattice spacings reflected by the selected and the corresponding UV-Vis diffuse reflectance spectrum (DRS) shows that the sample has strong absorption both in ultraviolet and visible-light regions, showing the penitential as a highly efficient photocatalyst (Fig. S8). To prove the concept, the photocatalytic activities of the as-prepared Ag@Ag(DMSO)$_x$Cl nanobelts were evaluated by photodegradation of Rhodamine 6G (R6G) and methylene blue (MB) dyes under visible-light illumination (Fig. 3 A and B). Just as expected, it is obvious that the peaks of R6G dye molecules disappear when the reaction time is 16 min, which indicates the it had been decomposed thoroughly by the

Physical Chemistry Chemical Physics Accepted Manuscript

Ag@Ag(DMSO)$_x$Cl nanobelts product. In addition, the aqueous solution of MB molecules exhibits a double-peak feature at 667 and 612 nm, which correspond to monomers and dimers, respectively.[40] Illuminating the MB solution mixed with the Ag@Ag(DMSO)$_x$Cl nanobelts significantly bleaches both absorption peaks. However, the absorption peak at 612 nm becomes higher than the peak at 667 nm after 5 min, indicating that the degradation rate of monomers is much higher than that of dimers. When the reaction time is long enough, for example, 5.5 min, both monomers and dimers can be completely decomposed. The highly efficient photocatalytic properties achieved here demonstrate that the potential of as-prepared Ag@Ag(DMSO)$_x$Cl nanobelts could clean themselves under the SERS detection measurement.

Furthermore, the SERS detection performance of as-prepared nanobelts toward these two colorful molecules was investigated. Fig. 3C and D show the SERS spectra obtained from the samples treated in 10^{-5} M refresh R6G and MB solution, respectively. The Raman bands at about 1649, 1509, 1360, 1310, and 1190 cm^{-1} can be attributed to R6G and agree well with literature datas.[13, 41] In detail, the characteristic peaks at 1360, 1509 and 1649 cm^{-1} represent the carbon skeleton stretching modes of R6G, and the bands at 1182, and 1310 cm^{-1} are assigned to the C–C stretching and C–O–C stretching vibrations, respectively. The vibrational features of MB at around 1601 and 1386 cm^{-1} are attributed to the C-C and C-H stretching. Thus, just as expected, apart from the excellent photocatalytic properties, this Ag@Ag(DMSO)$_x$Cl nanobelts also exhibit the function of SERS detection, demonstrating that the potential of as-prepared Ag@Ag(DMSO)$_x$Cl nanobelts could be used as a recyclable SERS-active substrate.

As a proof of the concept, the SERS spectra of R6G and MB dye molecules were collected with the increasing excitation time. It can be seen that the intensities of the peaks decrease gradually, and the characteristic vibration peaks of R6G and MB nearly disappear after the illumination of 35 and 70 s, respectively. This phenomenon could be derived from the following three possibilities: 1) self-decomposition of the color dyes; 2) losing effectiveness of the SERS substrates; 3) photodegradation of the dye molecules. To clarify which factor dominating the results, firstly, the solid R6G and MB samples were measured without the Ag@Ag(DMSO)$_x$Cl nanobelts substrates (Fig. S9). Although the intensities is weak without enhanced substrate, it shows no obvious decay with the increased excitation time, demonstrating color dyes are difficult to self-decomposed. Meanwhile, the peak positions of the probe molecules shift a little compared with that collected with SERS substrates, and this should be ascribed to the chemical interaction effects between the dye molecules and the Ag@Ag(DMSO)$_x$Cl nanobelts. Moreover, to further study the self-cleaning mechanism of as-prepared Ag@Ag(DMSO)$_x$Cl nanobelts, the laser power and laser wavelength dependence of the R 6G SERS signals was investigated. As shown in Fig. S11, the higher laser power benefits the higher self-cleaning rate toward the R 6G molecule. Moreover, the Ag@Ag(DMSO)xCl nanobelts exhibit higher photocatalytic abilities under the excitation wavelength of 514 nm than that with 633 nm and 647 nm. This phenomenon should be attributed to the plasmonic effect of Ag cluster on the surface of the Ag(DMSO)xCl nanobelts, and it is consistent with the DRS spectrum of Ag@Ag(DMSO)xCl with a weak absorbance peak around ~520 nm. Thus, the Ag@Ag(DMSO)xCl nanobelts is a plasmonic photocatalyst.

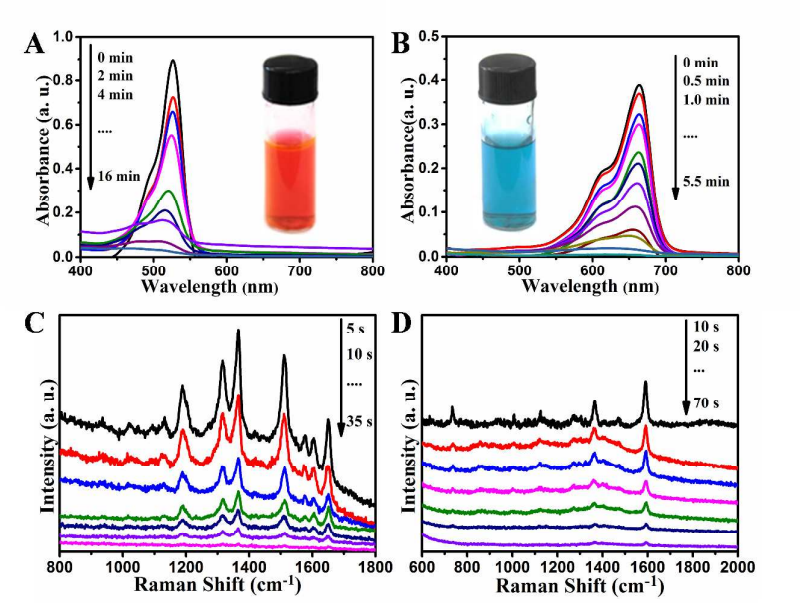

Fig. 3 UV-vis absorbance spectra of R6G (A) and MB (B) dye molecules after irradiation for different time in the presence of Ag@Ag(DMSO)$_x$Cl nanobelts. SERS spectra of R6G (C) and MB (D) under uninterrupted measurement using Ag@Ag(DMSO)$_x$Cl nanobelts as the active substrates.

This journal is © The Royal Society of Chemistry 20xx

Please do not adjust margins

Physical Chemistry Chemical Physics Accepted Manuscript

Then, a series of in-situ experiments were carried out to test the recyclability of the substrate. At the beginning, a free-standing Ag@Ag(DMSO)$_x$Cl nanobelts film prepared via the suction filtration method, were cut into small pieces and then seperated onto a marked silicon sheet to fix position of each detection, as shown in Fig. 4 A-C. After target molecules adsorbing onto the substrate, the SERS spectra show obvious characterized peaks of R6G and MB, and they decay gradually with the continuous excitation during the in-situ SERS detection measurement. The strongest peak intensity at 1509 cm^{-1} of R6G and 1601 cm^{-1} of MB were chosen as references for the spectra normalization, respectively, and after 35 s and 70 s, the signals of fresh R6G and MB molecules nearly disappeared. Then after redroping the targeted molecules onto the substrate, the SERS detection measurement was carried out in-situ, and it is interesting to see that the characteristic vibration peaks come out and decrease gradually with the increased illumination times once again, demonstrating the Ag@Ag(DMSO)$_x$Cl nanobelts substrate do not lose its effectiveness and is recyclable. Furthermore, the in-situ SERS detection (Fig. 4 D and E) is repeatedly measured several times, and the spectra for both R6G and MB molecules show no obvious difference during each cycle. Based on the above results, it can be concluded that the probe molecules should have been photodegratated during the SERS detection measurement. Thus, the Ag@Ag(DMSO)$_x$Cl nanobelts substrate can self-clean during the SERS detection process.

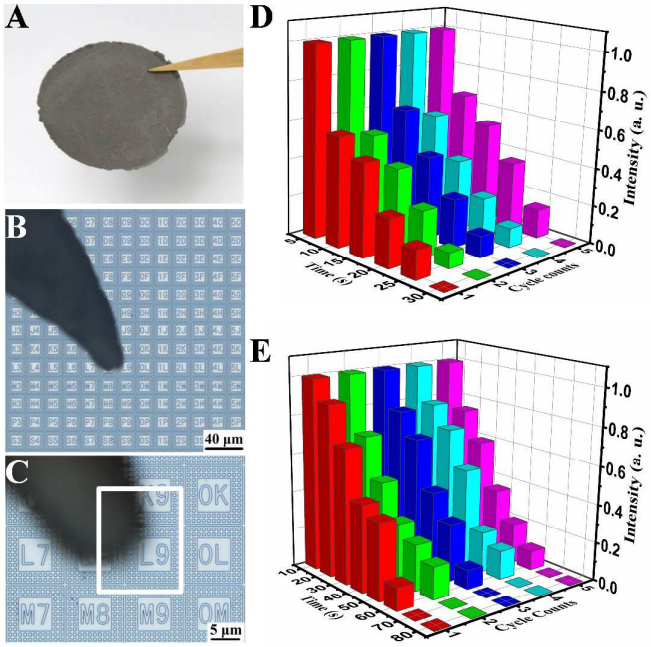

Fig. 4 (A) Photo image of the Ag@Ag(DMSO)$_x$Cl film prepared *via* vacuum filtration. (B, C) The as-prepared substrate placed on a marked silicon sheet for in-situ SERS detection. Reversible SERS behavior of Ag@Ag(DMSO)$_x$Cl nanobelts with five cycles: R6G (D) and MB (E).

Conclusions

In summary, Ag@Ag(DMSO)$_x$Cl nanobelts have been successfully prepared for the first time via a dissolution and recrytalline process. They exhibit excellent photocatalytic properties and highly sensitive SERS detection activities toward target organic molecules. An active substrates assembled by these inorganic-organic hybrid nanobelts can achieve its ultrafast self-cleaning by the photodegredation of probe molecules during the in-situ SERS detection process, and thus realize the renewability spontaneously, showing the potential for the real-time online monitoring. Our work presented here is superior to traditionally recyclable SERS-active substrates which need compulsorily time-consuming and complex procedures, and provide a new strategy to design and fabricate reproducible SERS-active sbustrate.

Acknowledgements

This work was supported by the Natiaoal Key Basic Research Program of China (2014CB31802), National Natural Science Foundation of China (11079002) and the Fundamental Research Funds For the Central Universities (30428201).

Notes and references

1. M. Moskovits, *Nature*, 2010, **464**, 357.
2. M. D. Porter, R. J. Lipert, L. M. Siperko, G. Wang and R. Narayanan, *Chem. Soc. Rev.*, 2008, **37**, 1001.
3. Y. C. Cao, R. Jin and C. A. Mirkin, *Science*, 2002, **297**, 1536.
4. W. E. Smith, *Chem. Soc. Rev.*, 2008, **37**, 955.

Physical Chemistry Chemical Physics Accepted Manuscript

5. W. Li, P. H. C. Camargo, X. Lu and Y. Xia, *Nano Lett.*, 2009, **9**, 485.
6. X. Li, G. Chen, L. Yang, Z. Jin and J. Liu, *Adv. Funct. Mater.*, 2010, **20**, 2815.
7. L. Yang, Z. Bao, Y. Wu and J. Liu, *J. Raman Spectrosc.*, 2012, **43**, 848.
8. Z. Zheng, B. Huang, J. Lu, Z. Wang, X. Qin, X. Zhang, Y. Dai and M. H. Whangbo, *Chem. Commun.*, 2012, **48**, 5733.
9. X. Chen and S. S. Mao, *ChemInform*, 2007, **38**, 2891.
10. G. Liu, Y. Zhao, C. Sun, F. Li, G. Q. Lu and H. M. Cheng, *Angew. Chem. Int. Ed.*, 2008, **47**, 4516.
11. P. Xu, T. Xu, J. Lu, S. Gao, N. S. Hosmane, B. Huang, Y. Dai and Y. Wang, *Energy Environ. Sci.*, 2010, **8**, 1128.
12. E. Boisselier and D. Astruc, *Chem. Soc. Rev.*, 2009, **38**, 1759.
13. A. M. Michaels, M. Nirmal and L. E. Brus, *J. Am. Chem. Soc.*, 1999, **121**, 9932.
14. Y. Fang, N.H. Seong and D. D. Dlott, *Science*, 2008, **321**, 388.
15. P. Guyot-Sionnest, *J. Phys. Chem. B*, 2004, **108**, 5882.
16. A. Musumeci, D. Gosztola, T. Schiller, N. M. Dimitrijevic, V. Mujica, D. Martin and T. Rajh, *J. Am. Chem. Soc.*, 2009, **131**, 6040.
17. Y. Ye, J. Chen, Q. Ding, D. Lin, R. Dong, L. Yang and J. Liu, *Nanoscale*, 2013, **5**, 5887.
18. K. Liu, D. Li, R. Li, Q. Wang, S. Pan, W. Peng and M. Chen, *J. Mater. Res.*, 2013, **28**, 3374.
19. Z. Zheng, B. Huang, X. Qin, X. Zhang, Y. Dai and M. H. Whangbo, *J. Mater. Chem.*, 2011, **25**, 9079.
20. K. S. Lee and M. A. El-Sayed, *J. Phys. Chem. B*, 2006, **110**, 19220.
21. W. Hou and S. B. Cronin, *Adv. Funct. Mater.*, 2013, **23**, 1612.
22. H. Wei and H. Xu, *Nanoscale*, 2013, **22**, 10794.
23. Z. Zhang, S. Sheng, H. Zheng, H. Xu and M. Sun, *Nanoscale*, 2014, **9**, 4903.
24. P. Wang, B. Huang, X. Qin, X. Zhang, Y. Dai, J. Wei and M. H. Whangbo, *Angew. Chem. Int. Ed.*, 2008, **47**, 7931.
25. H. Wang, J. Yang, X. Li, H. Zhang, J. Li and L. Guo, *Small*, 2012, **8**, 2802.
26. H. Wang, J. Gao, T. Guo, R. Wang, L. Guo, Y. Liu and J. Li, *Chem. Commun.*, 2012, **48**, 275.
27. H. Wang, Y. S. Bai, J. Yang, X. F. Lang, J. Li and L. Guo, *Chem. Eur. J.*, 2012, **18**, 5524.
28. Y. Bi, S. Ouyang, N. Umezawa, J. Cao and J. Ye, *J. Am. Chem. Soc.*, 2011, **133**, 6490.
29. C. Han, L. Ge, C. Chen, Y. Li, Z. Zhao, X. Xiao, Z. Li and J. Zhang, *J. Mater. Chem. A*, 2014, **31**, 12594.
30. C. An, S. Peng and Y. Sun, *Adv. Mater.*, 2010, **22**, 2570.
31. Y. Tang, Z. Jiang, G. Xing, A. Li, P. D. Kanhere, Y. Zhang, T. C. Sum, S. Li, X. Chen, Z. Dong and Z. Chen, *Adv. Funct. Mater.*, 2013, **23**, 2932.
32. Y. Wu, T. Hang, J. Komadina, H. Ling and M. Li, *Nanoscale*, 2014, **16**, 9720.
33. H. W. Liang, J. W. Liu, H. S. Qian and S. H. Yu, *Acc. Chem. Res.*, 2013, **46**, 1450.
34. J. W. Liu, H. W. Liang and S. H. Yu, *Chem. Rev.*, 2012, **112**, 4770.
35. Y.Z. Long, M. Yu, B. Sun, C. Z. Gu and Z.Fan, *Chem. Soc. Rev.*, 2012, **12**, 4560.
36. A. R. Tao, J. Huang and P. Yang, *Acc. Chem. Res.*, 2008, **41**, 1662.
37. K. Yoon, B. S. Hsiao and B. Chu, *J. Mater. Chem.*, 2008, **44**, 5326.
38. S. P. Sharma and S. C. Lahiri, *Spectrochim. Acta, Pt. A: Mol. Biomol. Spectrosc.*, 2008, **70**, 144.
39. D. P. Wang, P. D. B. Huang, P. X. Zhang, X. Qin, P. D. Y. Dai, D. Z. Wang and Z. Lou, *ChemCatChem*, 2011, **3**, 360.
40. F. T. Zhang, J. Nie, D. W. Zhang, J. T. Chen, Y. L. Zhou and X. X. Zhang, *Anal. Chem.*, 2014, **86**, 9489
41. D. Pristinski, S. Tan, M. Erol, H. Du and S. Sukhishvili, *J. Raman Spectrosc.*, 2006, **37**, 762.

Physical Chemistry Chemical Physics Accepted Manuscript

This journal is © The Royal Society of Chemistry 20xx

Please do not adjust margins